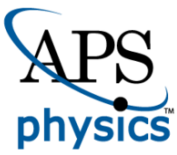

Nucleon form factors and spin content in a quark-diquark model with a pion cloud

Ian C. Cloët and Gerald A. Miller

Phys. Rev. C **86**, 015208 — Published 18 July 2012

DOI: 10.1103/PhysRevC.86.015208

Nucleon form factors and spin content in a quark-diquark model with a pion cloud

Ian C. Cloët[1,2] and Gerald A. Miller[1]

[1] *Department of Physics, University of Washington, Seattle, WA 98195-1560, USA*
[2] *The Special Research Centre for the Subatomic Structure of Matter, School of Chemistry and Physics University of Adelaide, Adelaide SA 5005, Australia*

We propose a new model of the nucleon in which quark-diquark configurations immersed in a pion cloud are treated in a manner consistent with Poincaré invariance. With suitably chosen parameters, the computations employing this model reproduce the measured electromagnetic form factors and the quark-spin contribution to the total nucleon angular momentum.

PACS numbers: 12.39.Ki, 13.40.Gp, 14.20.Dh
Keywords: nucleon elastic form factors, nucleon spin-sum

I. INTRODUCTION

The nucleon is the lightest baryon and its mass dominates the nucleus, which is the heart of the atom. Quantum chromodynamics tells us that the nucleon is a complex system composed of three valence quarks and an undefined number of quark-antiquark pairs and gluons. Deep inelastic scattering measurements have demonstrated that the sum of the spins of the quarks do not add up to the total angular momentum of the nucleon [1]. This puzzle has been the subject of a tremendous amount of experimental and theoretical investigation. Another probe of the structure of the nucleon is elastic electron-nucleon scattering. Measurements made at Jefferson Lab have shown that the proton form factor ratio, $G_{Ep}(Q^2)/G_{Mp}(Q^2)$, decreases as the value of Q^2 is increased above about 1 GeV^2. This important discovery renewed interest in the structure of the nucleon.

The present paper is devoted to answering a simple question: can a model of the nucleon which consists of three valence quarks and a pion cloud, constrained by Poincaré invariance, describe the existing data for elastic electromagnetic form factors, while properly accounting for the small fraction of the proton total angular momentum carried by the quarks. Recent work indicates that the successful construction of such a model should be possible [2], provided the model quark wave functions have suitable properties.

The challenge of understanding nucleon elastic form factors has been taken up by many, for example, see the review [3] and Ref. [4]. Here we follow only one particular line of reasoning. The light-front model of Ref. [5], with three constituent quarks, was used to predict the fall of the ratio $G_{Ep}(Q^2)/G_{Mp}(Q^2)$. The effects of the pion cloud were later included [6, 7], and this led to a reasonably accurate description of all four electromagnetic form factors. However, the quarks in the bare nucleon carry about 75% of the total angular momentum of the nucleon, which is too large to reproduce the measured value of approximately 30%. Furthermore, the computed ratio $G_{Ep}(Q^2)/G_{Mp}(Q^2)$ falls a little too rapidly with increasing values of Q^2, and the results were not completely consistent with the detailed flavor decomposition of the empirical form factors [8]. This earlier work on the proton form factors was carried out with a very simple three-quark wave function. In the present work we use a more sophisticated wave function, consisting of a quark-scalar-diquark term and a quark-axial-vector-diquark term, with two invariant forms for each term.

The plan of the paper is as follows: Sect. II is devoted to a complete description of the model, including the light-front wave function (LFWF) and the addition of the pion cloud, along with the formalism necessary to compute observable quantities. The parameters of the model are discussed in Sect. III, where they are varied to describe the existing data for nucleon electromagnetic form factors. The choice of parameters completes the definition of the model. The model is tested in Sect. IV by computing the quark contribution to the nucleon spin and Sect. V is reserved for a summary and discussion.

II. A COVARIANT LIGHT-FRONT MODEL FOR THE NUCLEON

The basic model is that the valence quarks, represented by quark-diquark combinations with the quantum numbers of the nucleon, are immersed in a cloud of pions. The motivation for this idea is obvious. We know that the nucleon is made of quarks and that there is a long range interaction between nucleons mediated by the exchange of a single pion. However, a pion emitted by a nucleon can be absorbed by the same nucleon, so each nucleon has a pion cloud. The low mass of the pion is the reason for singling it out as the only meson to be treated separately as a cloud [9]. As we shall see, including the pion cloud leads to a significant reduction in the fraction of the nucleons total angular momentum carried by the quark spin, and this is consistent with previous findings [2, 10]. We use the light-front representation of the nucleon wave function [11] to guarantee that the observable quantities have the appropriate properties under Lorentz transformations. The remainder of this section details how this is done.

In general, the light-front wave function (LFWF) of a hadron with spin projection $J_z = \pm\frac{1}{2}$ is represented by

the function $\Psi^{J_z}_{\lambda_1,\ldots,\lambda_n}(x_i, \boldsymbol{k}_{\perp i})$ [11], where

$$k_i = \left(k_i^+, k_i^-, \boldsymbol{k}_{\perp i}\right) = \left(x_i\, p^+, \tfrac{\boldsymbol{k}_{\perp i}^2 + m_i^2}{x_i\, p^+}, \boldsymbol{k}_{\perp i}\right), \quad (1)$$

specifies the 4-momentum of each constituent and λ_i specifies its light-front helicity in the z-direction. The light-front momentum fractions, $x_i = \frac{k_i^+}{p^+}$, are all positive and satisfy $\sum_i x_i = 1$. The scalar parts of the LFWF are functions of the Lorentz invariant quantities x_i and the invariant mass squared, M_0^2, given by

$$M_0^2 = \sum_i^n \frac{\boldsymbol{k}_{\perp i}^2 + m_i^2}{x_i} = \Big(\sum\nolimits_i k_i\Big)^2, \quad (2)$$

where m_i is the mass of each nucleon constituent.

For a nucleon that consists of two constituents, in our case a quark and a diquark, the nucleon Fock state can be expressed as

$$\left|p^+, \boldsymbol{p}_\perp = 0,\, \lambda\right\rangle = \int \frac{dx\, d^2k_\perp}{16\pi^3\sqrt{x(1-x)}} \sum_{\lambda_q,\lambda_a} \Psi^\lambda_{\lambda_q\lambda_a}(x, \boldsymbol{k}_\perp) \left|xp^+, \boldsymbol{k}_\perp, \lambda_q, \lambda_a\right\rangle, \quad (3)$$

where $\Psi^\lambda_{\lambda_q\lambda_a}(x, \boldsymbol{k}_\perp)$ is the LFWF that describes the interaction of a quark and a diquark to form a nucleon. We have chosen a frame where the transverse momentum of the nucleon is zero, and the helicities of the quark and diquark states are labeled by λ_q and λ_a, respectively. The two particle Fock-state ket in Eq. (3) is defined by

$$\left|xp^+, \boldsymbol{k}_\perp, \lambda_q, \lambda_a\right\rangle \equiv \left|k_1^+ = x\, p^+, k_2^+ = (1-x)p^+, k_{1\perp} = k_\perp, k_{2\perp} = -k_\perp; \lambda_q, \lambda_a\right\rangle. \quad (4)$$

In this work we make the quark-diquark approximation for the LFWF of the nucleon, where we include both scalar and axial-vector diquark correlations. The LFWF then takes the form

$$\Phi^\lambda_{\lambda_q\,\lambda_a}(k,p) = \bar u_q(k,\lambda_q)\left[\varphi_1^s + \frac{M\,\not\omega}{\omega\cdot p}\varphi_2^s\right] u(p,\lambda) + \bar u_q(k,\lambda_q)\,\varepsilon^*_\nu(q,\lambda_a)\gamma^\nu\gamma_5\left[\varphi_1^a + \frac{M\,\not\omega}{\omega\cdot p}\varphi_2^a\right] u(p,\lambda), \quad (5)$$

where the first term represents correlations in the quark–scalar-diquark channel and the second quark–axial-vector-diquark correlations. The variables k, q, p are respectively the quark, diquark and nucleon momentum, where $p = k + q$ and M is the nucleon mass. The quark and nucleon spinors are represented by $u_q(k,\lambda_q)$ and $u(p,\lambda)$, respectively, and $\varepsilon^\mu(q,\lambda_a)$ is the usual spin-one polarization vector, representing the spin-one axial-vector diquark. The interaction of the quark with the diquark, in each diquark channel, is encapsulated by two scalar functions, namely φ_1 and φ_2. We choose the φ_1 and φ_2 scalar functions to have the form

$$\varphi_1 = \frac{1}{(M_0^2 + \beta^2)^\gamma}, \qquad \varphi_2 = c\,\frac{(M_0 - M)}{2\,M}\varphi_1. \quad (6)$$

This choice is motivated by the success of earlier work described in Ref. [12].

The wave function given in Eq. (5) is defined at the light-front plane $\omega\cdot x = \sigma$, where ω is a light-like vector. For a stationary state we can consider a fixed light-cone time and set $\sigma = 0$. The usual choice for the quantization direction is $\omega = (1,0,0,-1)$, so the nucleon wave function becomes

$$\Phi^\lambda_{\lambda_q\,\lambda_a}(k,p) = \phi^\lambda_{\lambda_q}(k,p) + \phi^\lambda_{\lambda_q\,\lambda_a}(k,p), = \bar u_q(k,\lambda_q)\left[\varphi_1^s + \frac{M}{p^+}\gamma^+\varphi_2^s\right] u(p,\lambda) + \bar u_q(k,\lambda_q)\,\varepsilon^*_\nu(q,\lambda_a)\gamma^\nu\gamma_5\left[\varphi_1^a + \frac{M}{p^+}\gamma^+\varphi_2^a\right] u(p,\lambda), \quad (7)$$

where $\phi^\lambda_{\lambda_q}(k,p)$ represents the quark–scalar-diquark component and $\phi^\lambda_{\lambda_q\,\lambda_a}(k,p)$ the quark–axial-vector-diquark component of the nucleon LFWF. The above wave function contains only the spin couplings, therefore to fully define the model we also need the flavor couplings. The flavor wave function of the proton is given by

$$|p\rangle = \frac{1}{\sqrt{2}}|u\,S\rangle + \frac{1}{\sqrt{6}}|u\,T_0\rangle - \frac{1}{\sqrt{3}}|d\,T_1\rangle, \quad (8)$$

where S is the flavor singlet state and T the flavor triplet and therefore we obtain a symmetric spin-flavor wavefunction. The anti-symmetrization inherent in the model is represented by Eq. (8), where any one of the three quarks can be the $u\,, u\,, d$ of the three terms in that equation.

A. Bare nucleon form factors

For on-shell initial and final nucleon states, the Dirac and Pauli electromagnetic form factors of the nucleon are defined via the matrix element decomposition

$$\langle p',\,\lambda'\,|J^\mu_{\rm em}|\,p,\,\lambda\rangle = \bar u(p',\lambda')\left[\gamma^\mu\,F_1(Q^2) + \frac{i\sigma^{\mu\nu}q_\nu}{2\,M}\,F_2(Q^2)\right] u(p,\lambda), \quad (9)$$

where M is the nucleon mass and $Q^2 = -q^2$, where q is the 4-momentum transfer. We choose to work in the Drell-Yan-West frame, where the light-front momentum decompositions of the relevant 4-vectors are

$$q = \left(q^+, q^-, \boldsymbol{q}_\perp\right) = \left(0, \tfrac{Q^2}{p^+}, \boldsymbol{q}_\perp\right), \quad (10)$$

$$p = \left(p^+, p^-, \boldsymbol{p}_\perp\right) = \left(p^+, \tfrac{M^2}{p^+}, \boldsymbol{0}_\perp\right), \quad (11)$$

so that $q^2 = -2\,p\cdot q = -\boldsymbol{q}_\perp^2 = -Q^2$. With this choice the Dirac and Pauli from factors are identified with the helicity-conserving and helicity-flip matrix elements of the plus-component of the electromagnetic current, that is

$$F_1(Q^2) = \frac{1}{2\,p^+}\,\langle p',\uparrow\,|J^+_{\rm em}|\,p,\uparrow\rangle\,, = \frac{1}{2\,p^+}\,\langle p',\downarrow\,|J^+_{\rm em}|\,p,\downarrow\rangle\,, \quad (12)$$

$$F_2(Q^2) = \frac{-2\,M}{(q^1 - iq^2)}\,\frac{1}{2\,p^+}\,\langle p',\uparrow|\,J^+_{\rm em}\,|p,\downarrow\rangle\,,$$
$$= \frac{2\,M}{(q^1 + iq^2)}\,\frac{1}{2\,p^+}\,\langle p',\downarrow|\,J^+_{\rm em}\,|p,\uparrow\rangle\,. \quad (13)$$

To determined the nucleon form factors we must therefore compute the above matrix elements of the J^+ component of the electromagnetic current.

Using Eq. (3) and the matrix element definitions of the nucleon form factors given in Eqs. (12) and (13), it is clear that the nucleon form factors are given by

$$F_1(Q^2) = \int \frac{dx\,d^2k_\perp}{\sqrt{x(1-x)}} \times \sum_{\lambda_q,\,\lambda_a=+,-} \Psi^{\uparrow *}_{\lambda_q,\,\lambda_a}(x,\boldsymbol{k}'_\perp)\Psi^{\uparrow}_{\lambda_q,\,\lambda_a}(x,\boldsymbol{k}_\perp), \quad (14)$$

$$F_2(Q^2) = \frac{2\,M}{q^1 + iq^2}\int \frac{dx\,d^2k_\perp}{\sqrt{x(1-x)}} \times \sum_{\lambda_q,\,\lambda_a=+,-} \Psi^{\downarrow *}_{\lambda_q,\,\lambda_a}(x,\boldsymbol{k}'_\perp)\Psi^{\uparrow}_{\lambda_q,\,\lambda_a}(x,\boldsymbol{k}_\perp). \quad (15)$$

The helicity components of the LFWFs for scalar and axial-vector diquarks are defined via

$$\psi^{\lambda}_{\lambda_q}(x,\boldsymbol{k}_\perp) = \frac{1}{\sqrt{x(1-x)}}\,\phi^{\lambda}_{\lambda_q}(k,p), \quad (16)$$

$$\psi^{\lambda}_{\lambda_q\,\lambda_a}(x,\boldsymbol{k}_\perp) = \frac{1}{\sqrt{x(1-x)}}\,\phi^{\lambda}_{\lambda_q\,\lambda_a}(k,p), \quad (17)$$

and for convenience we define the scalar functions

$$f^s_1(Q^2) = \int \frac{dx\,d^2k_\perp}{16\pi^3} \sum_{\lambda_q=+,-} \psi^{\uparrow *}_{\lambda_q}(x,\boldsymbol{k}'_\perp)\psi^{\uparrow}_{\lambda_q}(x,\boldsymbol{k}_\perp), \quad (18)$$

$$f^a_1(Q^2) = \int \frac{dx\,d^2k_\perp}{16\pi^3} \times \sum_{\lambda_q,\,\lambda_a=+,-} \psi^{\uparrow *}_{\lambda_q,\,\lambda_a}(x,\boldsymbol{k}'_\perp)\psi^{\uparrow}_{\lambda_q,\,\lambda_a}(x,\boldsymbol{k}_\perp), \quad (19)$$

$$f^s_2(Q^2) = \frac{2M}{q^1 + i\,q^2}\int \frac{dx\,d^2k_\perp}{16\pi^3} \times \sum_{\lambda_q=+,-} \psi^{\downarrow *}_{\lambda_q}(x,\boldsymbol{k}'_\perp)\psi^{\uparrow}_{\lambda_q}(x,\boldsymbol{k}_\perp), \quad (20)$$

$$f^a_2(Q^2) = \frac{2M}{q^1 + i\,q^2}\int \frac{dx\,d^2k_\perp}{16\pi^3} \times \sum_{\lambda_q,\,\lambda_a=+,-} \psi^{\downarrow *}_{\lambda_q,\,\lambda_a}(x,\boldsymbol{k}'_\perp)\psi^{\uparrow}_{\lambda_q,\,\lambda_a}(x,\boldsymbol{k}_\perp). \quad (21)$$

Using the flavor wave function given in Eq. (8), the quark flavor contributions to the bare (without pion cloud) proton Dirac form factor are therefore given by

$$F^{(0),u}_{1p}(Q^2) = \frac{3}{2}\,e_u\,f^s_1(Q^2) + \frac{1}{2}\,e_u\,f^a_1(Q^2), \quad (22)$$

$$F^{(0),d}_{1p}(Q^2) = e_d\,f^a_1(Q^2), \quad (23)$$

where e_u and e_d are the quark charges and analogous expressions hold for the quark flavor contributions to the Pauli form factors, with $f^s_1 \to f^s_2$ and $f^a_1 \to f^a_2$. The scalar functions $f^s_1(Q^2)$ and $f^a_1(Q^2)$ are subject to the normalizations $f^s_1(0) = 1 = f^a_1(0)$, which guarantees the correct quark and hence nucleon charges. Using charge symmetry we obtain the following results for the bare nucleon Dirac form factors

$$F^{(0)}_{1p}(Q^2) = \frac{3}{2}\,e_u\,f^s_1(Q^2) + \frac{1}{2}\,(e_u + 2\,e_d)\,f^a_1(Q^2),$$
$$= f^s_1(Q^2), \quad (24)$$

$$F^{(0)}_{1n}(Q^2) = \frac{3}{2}\,e_d\,f^s_1(Q^2) + \frac{1}{2}\,(e_d + 2\,e_u)\,f^a_1(Q^2),$$
$$= -\frac{1}{2}\,f^s_1(Q^2) + \frac{1}{2}\,f^a_1(Q^2), \quad (25)$$

where again analogous expressions hold for the Pauli form factors, with $f^s_1 \to f^s_2$ and $f^a_1 \to f^a_2$.

Using the LFWF given in Eq. (7) and the definition given in Eq. (16), the explicit form of the scalar diquark helicity components of the LFWFs are

$$\sqrt{(1-x)}\,\psi^{\uparrow}_{+}(x,\boldsymbol{k}_\perp) = \left(M + \frac{m}{x}\right)\varphi^s_1 + 2\,M\,\varphi^s_2, \quad (26)$$

$$\sqrt{(1-x)}\,\psi^{\uparrow}_{-}(x,\boldsymbol{k}_\perp) = -\frac{1}{x}\,(k^1 + i\,k^2)\,\varphi^s_1, \quad (27)$$

$$\sqrt{(1-x)}\,\psi^{\downarrow}_{+}(x,\boldsymbol{k}_\perp) = \frac{1}{x}\,(k^1 - i\,k^2)\,\varphi^s_1, \quad (28)$$

$$\sqrt{(1-x)}\,\psi^{\downarrow}_{-}(x,\boldsymbol{k}_\perp) = \left(M + \frac{m}{x}\right)\varphi^s_1 + 2\,M\,\varphi^s_2. \quad (29)$$

Similarly, using Eq. (7) and the definition given in Eq. (17), the helicity components of the LFWFs for axial-vector diquark are

$$\sqrt{(1-x)}\,\psi^{\uparrow}_{++}(x,\boldsymbol{k}_\perp) = \frac{\sqrt{2}\,(k^1 - i\,k^2)}{x(1-x)}\varphi^a_1, \quad (30)$$

$$\sqrt{(1-x)}\,\psi^{\uparrow}_{-+}(x,\boldsymbol{k}_\perp) = \sqrt{2}\left(M + \frac{m}{x}\right)\varphi^a_1 + 2\sqrt{2}\,M\,\varphi^a_2, \quad (31)$$

$$\sqrt{(1-x)}\,\psi^{\uparrow}_{+-}(x,\boldsymbol{k}_\perp) = -\frac{\sqrt{2}\,(k^1 + i\,k^2)}{1-x}\varphi^a_1, \quad (32)$$

$$\sqrt{(1-x)}\,\psi^{\uparrow}_{--}(x,\boldsymbol{k}_\perp) = 0, \quad (33)$$

and

$$\sqrt{(1-x)}\,\psi^{\downarrow}_{++}(x,\boldsymbol{k}_\perp) = 0, \quad (34)$$

$$\sqrt{(1-x)}\,\psi^{\downarrow}_{-+}(x,\boldsymbol{k}_\perp) = -\frac{\sqrt{2}\,(k^1 - i\,k^2)}{1-x}\varphi^a_1, \quad (35)$$

$$\sqrt{(1-x)}\,\psi^{\downarrow}_{+-}(x,\boldsymbol{k}_\perp) = -\sqrt{2}\left(M + \frac{m}{x}\right)\varphi^a_1 - 2\sqrt{2}\,M\,\varphi^a_2, \quad (36)$$

$$\sqrt{(1-x)}\,\psi^{\downarrow}_{--}(x,\boldsymbol{k}_\perp) = \frac{\sqrt{2}\,(k^1 + i\,k^2)}{x(1-x)}\varphi^a_1. \quad (37)$$

Using these results it is then straightforward to obtain expressions for the scalar functions defined in Eqs. (18)-(21), namely

$$f_1^s(Q^2) = \frac{1}{16\pi^3}\int \frac{dx\, d^2k_\perp}{x^2(1-x)} \left\{\left[\boldsymbol{k}_\perp^2 + (x\,M+m)^2 - \frac{1}{4}(1-x)^2Q^2\right]\varphi_1^s\,\varphi_1^{s\prime} + 2\,x\,M(x\,M+m)\,(\varphi_1^s\,\varphi_2^{s\prime} + \varphi_1^{s\prime}\,\varphi_2^s) + 4\,x^2\,M^2\,\varphi_2^s\,\varphi_2^{s\prime}\right\}, \quad (38)$$

$$f_1^a(Q^2) = \frac{1}{8\pi^3}\int \frac{dx\, d^2k_\perp}{x^2(1-x)} \left\{\frac{1+x^2}{(1-x)^2}\left[\boldsymbol{k}_\perp^2 - \frac{1}{4}(1-x)^2Q^2\right]\varphi_1^a\varphi_1^{a\prime} + (x\,M+m)^2\,\varphi_1^a\varphi_1^{a\prime} + 2\,x\,M\,(x\,M+m)\,(\varphi_1^a\varphi_2^{a\prime} + \varphi_1^{a\prime}\varphi_2^a) + 4\,x^2\,M^2\,\varphi_2^a\varphi_2^{a\prime}\right\}, \quad (39)$$

$$f_2^s(Q^2) = \frac{M}{8\pi^3}\int \frac{dx\, d^2k_\perp}{x^2(1-x)} \left[(1-x)(x\,M+m)\varphi_1^{s\prime}\,\varphi_1^s - 2x\,M\,\frac{\boldsymbol{k}_\perp\cdot\boldsymbol{q}_\perp}{Q^2}\,(\varphi_1^s\,\varphi_2^{s\prime} - \varphi_2^s\,\varphi_1^{s\prime}) + x(1-x)\,M\,(\varphi_1^s\,\varphi_2^{s\prime} + \varphi_2^s\,\varphi_1^{s\prime})\right], \quad (40)$$

$$f_2^a(Q^2) = -\frac{M}{4\pi^3}\int \frac{dx\, d^2k_\perp}{x(1-x)^2} \left[(1-x)(x\,M+m)\varphi_1^{a\prime}\,\varphi_1^a - 2x\,M\,\frac{\boldsymbol{k}_\perp\cdot\boldsymbol{q}_\perp}{Q^2}\,(\varphi_1^a\,\varphi_2^{a\prime} - \varphi_2^a\,\varphi_1^{a\prime}) + x(1-x)\,M\,(\varphi_1^a\,\varphi_2^{a\prime} + \varphi_2^a\,\varphi_1^{a\prime})\right], \quad (41)$$

where the prime refers to the final state wave functions. The invariant masses are then given by

$$M_0^2 = \frac{\left(\vec{k}_\perp \mp \frac{1}{2}(1-x)\vec{q}_\perp\right)^2 + m^2}{x} + \frac{\left(\vec{k}_\perp \mp \frac{1}{2}(1-x)\vec{q}_\perp\right)^2 + M_D^2}{1-x}, \quad (42)$$

where M_D is the diquark mass, being either a scalar or axial-vector diquark, and the minus sign is for the initial state and plus sign the final state. Recall that M is the nucleon mass and m the constituent quark mass.

B. Nucleon form factors with a pion cloud

The pion cloud component of our model for the nucleon is introduced via a single pion loop around our bare nucleon, as illustrated in Fig. 1 for the nucleon electromagnetic current. The first diagram represents the photon coupling to the bare nucleon, multiplied by $Z_{N\pi}$, which represents the probability that the nucleon is in a configuration without a pion cloud. The second diagram in Fig. 1 represents the photon coupling to the bare nucleon with a pion in the air, the photon coupling is given by

$$\Lambda^\mu(p',p) = \tfrac{1}{2}\,(1+\tau_3)\left[\gamma^\mu\,F_{1p}^{(0)}(Q^2) + \frac{i\sigma^{\mu\nu}q_\nu}{2\,M}\,F_{2p}^{(0)}(Q^2)\right] + \tfrac{1}{2}\,(1-\tau_3)\left[\gamma^\mu\,F_{1n}^{(0)}(Q^2) + \frac{i\sigma^{\mu\nu}q_\nu}{2\,M}\,F_{2n}^{(0)}(Q^2)\right], \quad (43)$$

where $F_{1p}^{(0)}(Q^2)$, $F_{2p}^{(0)}(Q^2)$, etc, are the bare nucleon form factors discussed in Sect. II A. The contribution of this second diagram to observable quantities is usually small. Finally, the third diagram in Fig. 1 represents the photon coupling to the pion in the loop, with a pion electromagnetic vertex given by

$$\Lambda_{ij}^\mu(p',p) = \varepsilon_{3ji}\;(p'+p)^\mu\;F_\pi(Q^2), \quad (44)$$

where the pion form factor has the form $F_\pi(Q^2) = \left[1+Q^2/\Lambda_\pi^2\right]^{-1}$ and we choose the standard value of $\Lambda_\pi^2 = 0.5\,\mathrm{GeV}^2$.

The complete expressions for the proton and neutron Dirac and Pauli form factors are then

$$F_{1p} = Z_{N\pi}\,F_{1p}^{(0)} + \left(\tfrac{1}{2}\,F_{1p}^{(0)} + F_{1n}^{(0)}\right)F_{1N}^{(N),\mathrm{vec}} + \left(\tfrac{1}{2}\,F_{2p}^{(0)} + F_{2n}^{(0)}\right)F_{1N}^{(N),\mathrm{ten}} + F_{1N}^{(\pi)}, \quad (45)$$

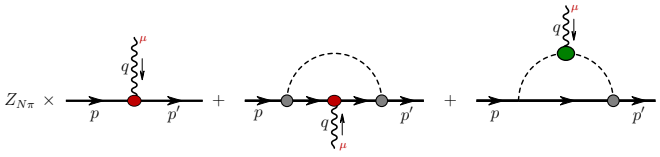

Figure 1. (Color online) Nucleon form factor diagrams, including the pion cloud. The multiplicative factor $Z_{N\pi}$ represents the probability that the nucleon is in a configuration without a pion cloud. In the second diagram the photon couples to the bare nucleon and in the third diagram it couples to the pion.

$$F_{1n}(Q^2) = Z_{N\pi}\, F_{1n}^{(0)} + \left(F_{1p}^{(0)} + \tfrac{1}{2}\, F_{1n}^{(0)}\right) F_{1N}^{(N),\rm vec} + \left(F_{2p}^{(0)} + \tfrac{1}{2}\, F_{2n}^{(0)}\right) F_{1N}^{(N),\rm ten}(Q^2) - F_{1N}^{(\pi)}, \quad (46)$$

$$F_{2p}(Q^2) = Z_{N\pi}\, F_{2p}^{(0)} + \left(\tfrac{1}{2}\, F_{1p}^{(0)} + F_{1n}^{(0)}\right) F_{2N}^{(N),\rm vec} + \left(\tfrac{1}{2}\, F_{2p}^{(0)} + F_{2n}^{(0)}\right) F_{2N}^{(N),\rm ten} + F_{2N}^{(\pi)}, \quad (47)$$

$$F_{2n}(Q^2) = Z_{N\pi}\, F_{2n}^{(0)} + \left(F_{1p}^{(0)} + \tfrac{1}{2}\, F_{1n}^{(0)}\right) F_{2N}^{(N),\rm vec} + \left(F_{2p}^{(0)} + \tfrac{1}{2}\, F_{2n}^{(0)}\right) F_{2N}^{(N),\rm ten} - F_{2N}^{(\pi)}, \quad (48)$$

where the Q^2 dependence of the various form factors has been omitted for clarity. The form factors $F_{1N}^{(N),\rm vec}(Q^2)$ and $F_{2N}^{(N),\rm vec}(Q^2)$ result from the second diagram in Fig. 1 where the photon couples to the bare nucleon with a γ^μ, while the form factors $F_{1N}^{(N),\rm ten}(Q^2)$ and $F_{2N}^{(N),\rm ten}(Q^2)$ arise from the $i\sigma^{\mu\nu}q_\nu$ coupling to the bare nucleon in the same diagram. Recall $F_{1p}^{(0)}$, $F_{1n}^{(0)}$, etc, are the bare nucleon form factors discussed in Sect. II A.

For the form factors arising from the pion loop in the second diagram of Fig. 1 we find [7]

$$F_{1N}^{(N),\rm vec}(Q^2) = g_{\pi N}^2 \int_0^1 dx \int \frac{d^2k_\perp}{2(2\pi)^3} F_{\pi N}(\boldsymbol{\ell}_+^2, x)\, F_{\pi N}(\boldsymbol{\ell}_-^2, x)\, \frac{x\left[\boldsymbol{k}_\perp^2 + x^2\, M^2 - \frac{1}{4}\, x^2\, Q^2\right]}{D^+(\boldsymbol{k}_\perp)\; D^-(\boldsymbol{k}_\perp)}, \quad (49)$$

$$F_{2N}^{(N),\rm vec}(Q^2) = -2\, g_{\pi N}^2\, M^2 \int_0^1 dx \int \frac{d^2k_\perp}{2(2\pi)^3} F_{\pi N}(\boldsymbol{\ell}_+^2, x)\, F_{\pi N}(\boldsymbol{\ell}_-^2, x)\, \frac{x^3}{D^+(\boldsymbol{k}_\perp)\; D^-(\boldsymbol{k}_\perp)}, \quad (50)$$

and

$$F_{1N}^{(N),\rm ten}(Q^2) = -g_{\pi N}^2\, \frac{1}{2} \int_0^1 dx \int \frac{d^2k_\perp}{2(2\pi)^3} F_{\pi N}(\boldsymbol{\ell}_+^2, x)\, F_{\pi N}(\boldsymbol{\ell}_-^2, x)\, \frac{x^3\, Q^2}{D^+(\boldsymbol{k}_\perp)\; D^-(\boldsymbol{k}_\perp)}, \quad (51)$$

$$F_{2N}^{(N),\rm ten}(Q^2) = -g_{\pi N}^2 \int_0^1 dx \int \frac{d^2k_\perp}{2(2\pi)^3} F_{\pi N}(\boldsymbol{\ell}_+^2, x)\, F_{\pi N}(\boldsymbol{\ell}_-^2, x)\, \frac{x\left[x^2\, M^2 - \frac{1}{4}\, x^2\, Q^2 + k_x^2 - k_y^2\right]}{D^+(\boldsymbol{k}_\perp)\; D^-(\boldsymbol{k}_\perp)}. \quad (52)$$

where we take $g_{\pi N} = 13.5$, $\boldsymbol{\ell}_\pm \equiv \boldsymbol{k}_\perp \pm \frac{1}{2}\, x\, \boldsymbol{q}_\perp$ and

$$D^\pm(\boldsymbol{k}_\perp) = \left(\boldsymbol{k}_\perp \pm \tfrac{1}{2}\, x\, \boldsymbol{q}_\perp\right)^2 + x^2\, M^2 + (1-x)\, m_\pi^2, \quad (53)$$

with m_π the pion mass. The pion-nucleon form factor that enters diagrams two and three in Fig. 1 is taken to be

$$F_{\pi N}\left(\ell_\perp^2, x\right) = e^{-\left[\ell_\perp^2 + x^2\, M^2 + (1-x) m_\pi^2\right] / \left[2x(1-x)\Lambda^2\right]}, \quad (54)$$

where Λ is a parameter that encapsulates the non-pointlike nature of the pion-nucleon vertex and will be determined in Sect. III. The form of $F_{\pi N}$ is chosen so as to maintain charge and momentum conservation [13]. An improvement was suggested in [33], but this has not yet been applied to calculating electromagnetic form factors.

The form factors arising from the pion loop in the third diagram of Fig. 1 are given by [7]

$$F_{1N}^{(\pi)} = g_{\pi N}^2\, F_\pi(Q^2) \int_0^1 dx \int \frac{d^2k_\perp}{(2\pi)^3} F_{\pi N}(\boldsymbol{k}_+^2, x)\, F_{\pi N}(\boldsymbol{k}_-^2, x) \frac{x\left[\boldsymbol{k}_\perp^2 - \frac{1}{4}(1-x)^2 Q^2 + x^2 M^2\right]}{D^+(\boldsymbol{k}_\perp)\; D^-(\boldsymbol{k}_\perp)}, \quad (55)$$

$$F_{2N}^{(\pi)} = 2\, g_{\pi N}^2\, M^2\, F_\pi(Q^2) \int_0^1 dx \int \frac{d^2k_\perp}{(2\pi)^3} F_{\pi N}(\boldsymbol{k}_+^2, x)\, F_{\pi N}(\boldsymbol{k}_-^2, x) \frac{x^2\,(1-x)}{D^+(\boldsymbol{k}_\perp)\; D^-(\boldsymbol{k}_\perp)}, \quad (56)$$

where we have defined

$$\boldsymbol{k}_\pm \equiv \boldsymbol{k}_\perp \pm \frac{1}{2}\,(1-x)\, \boldsymbol{q}_\perp. \quad (57)$$

We note that the present version provides a minimal treatment of the pion cloud. Effects of the intermediate Δ and terms involving a $\gamma N \to \pi N$ direct coupling are not included. Both of these terms involve distances smaller than those of the terms we do include, which dominate in the chiral limit. Therefore we shall assume that such effects are subsumed within the parameters of the model. We shall see that achieving the present modest goal of reproducing form factors, while remaining consistent with the small fraction of the nucleon total angular momentum carried by the quarks spin is possible without including terms additional to those of the above equations.

III. RESULTS FOR NUCLEON FORM FACTORS AND THEIR FLAVOR DEPENDENCE

The parameters of the model are as follows: the quark, scalar diquark and axial-vector diquark masses, labeled by m, M_s and M_a respectively; the three parameters c_s, β_s and γ_s (see Eq. (6)) that specify the quark–scalar-diquark component of the nucleons LFWF and the analogous three parameters c_a, β_a and γ_a which encapsulates the quark–axial-vector-diquark component of the nucleons LFWF. Finally, there is the parameter Λ which enters Eq. (54) and describes the high momentum transfer fall off of the pion-nucleon vertex function. Therefore, in total the model has ten parameters and these are chosen to

χ^2	m	M_s	M_a	c_s	β_s	γ_s	c_a	β_a	γ_a	Λ	μ_p (μ_N)	μ_n (μ_N)
0.078516	0.191	0.414	0.167	1.509	1.226	5.719	0.008	1.104	8.586	1.035	2.794	-1.849

Table I. Model parameters: m constituent quark mass, M_s scalar diquark mass, M_a axial vector diquark mass, quark–scalar-diquark nucleon LFWF parameters c_s, β_s , γ_s (see Eq. (6)), quark–axial-vector-diquark nucleon LFWF parameters c_a, β_a , γ_a (see Eq. (6)), pion-nucleon vertex parameter Λ (see Eq. (54)). All mass-dimensioned parameters are in GeV. The first column gives the χ^2 obtained in the fit expressed in Eq. (58) and the final two columns present our results for the proton and neutron magnetic moments.

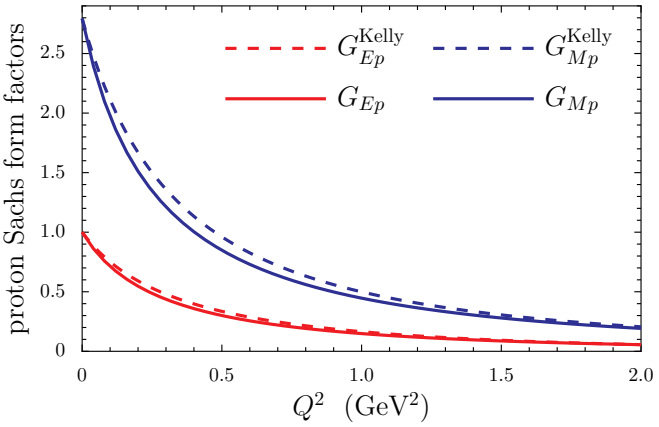

Figure 2. (Color online) Solid lines are the model results for the proton Sachs form factors and the dashed lines are the empirical results from Kelly given in Ref. [14].

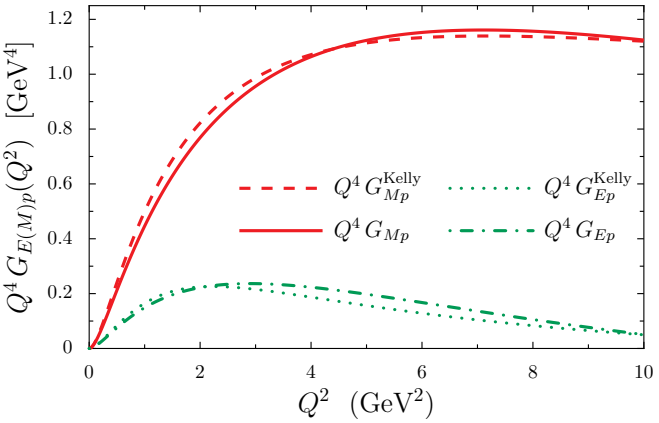

Figure 3. (Color online) Proton Sachs form factors and their comparison with the empirical parametrizations of Ref. [14].

minimize χ^2 as defined by

$$\chi^2 \equiv \frac{1}{4\,n_q}\sum_{Q^2}\left[\frac{|F_{1p}-F_{1p}^{\rm exp}|}{|F_{1p}^{\rm exp}|}+\frac{|F_{2p}-F_{2p}^{\rm exp}|}{|F_{2p}^{\rm exp}|}+\frac{|F_{1n}-F_{1n}^{\rm exp}|}{|F_{1n}^{\rm exp}|}+\frac{|F_{2n}-F_{2n}^{\rm exp}|}{|F_{2n}^{\rm exp}|}\right], \quad (58)$$

where F_{1p}, etc, are the form factors from the model, given in Eqs. (45)-(48), and for the empirical form factors, namely $F_{1p}^{\rm exp}$, etc, we take the results from Ref. [14]. For

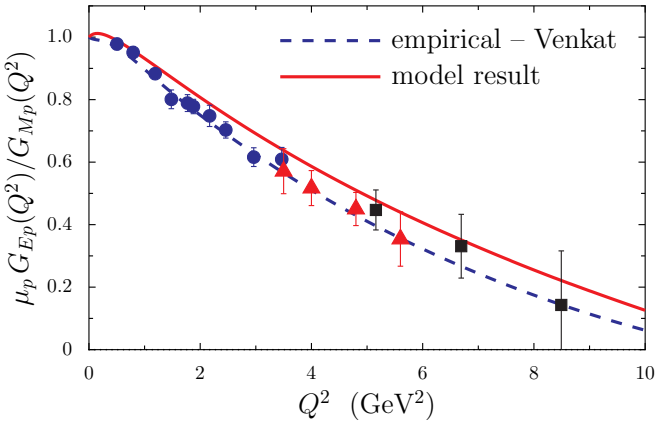

Figure 4. (Color online) Ratios of the proton electric to magnetic Sachs form factors. The solid curve is our model result and the dashed curve is the phenomenological fit of Ref. [15]. The data are from Refs. [16–20].

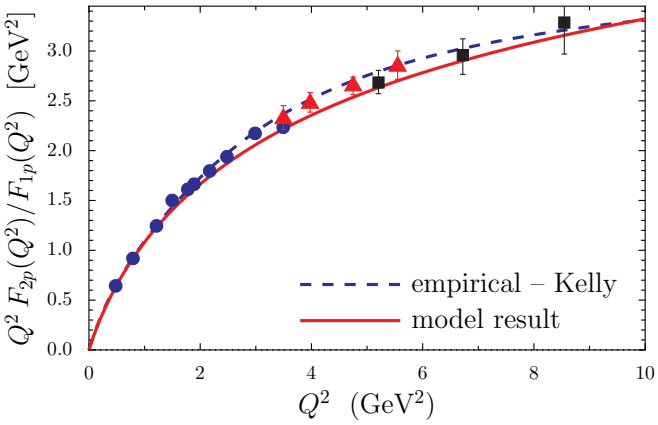

Figure 5. (Color online) Ratios of the proton Pauli to Dirac form factors multiplied by Q^2. The solid curve is our model result and the dashed curve is the empirical result of Ref. [14]. The data are from Refs. [16–20].

the sum in Eq. (58) we take n_q values of Q^2 chosen uniformly on the domain $Q^2 \in [0, 10]\,{\rm GeV}^2$ and Table III gives the resulting model parameters for $n_q = 11$. In this fit the resulting mass of the axial-vector diquark, namely $M_a = 167\,{\rm MeV}$, does not seem to be realistic. Such a small value could be the result of a surprisingly strong binding forces in that system. However, the small value may be masking the limitations of the spatial wave

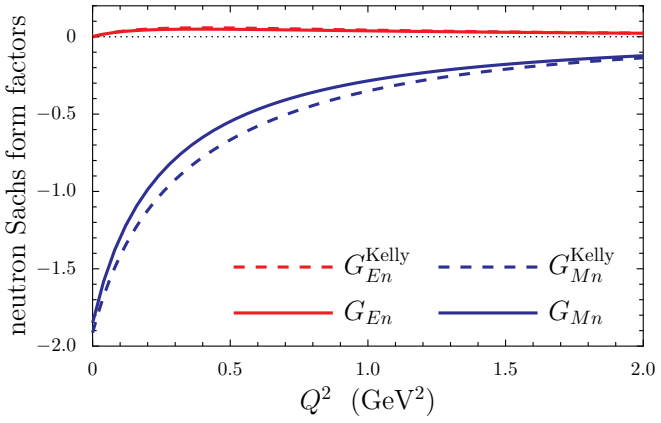

Figure 6. (Color online) Solid lines are the model results for the neutron Sachs form factors and the dashed lines are the empirical results from Kelly given in Ref. [14].

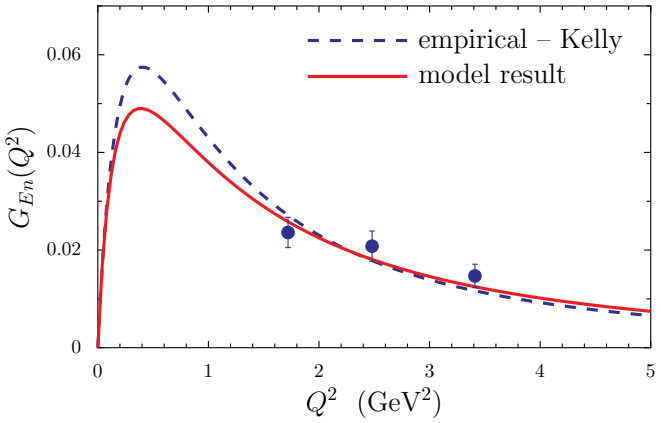

Figure 7. (Color online) The model result for the neutron Sachs electric form factor is given by the solid line and the dashed curves is from Kelly [14]. The data is from Ref. [21].

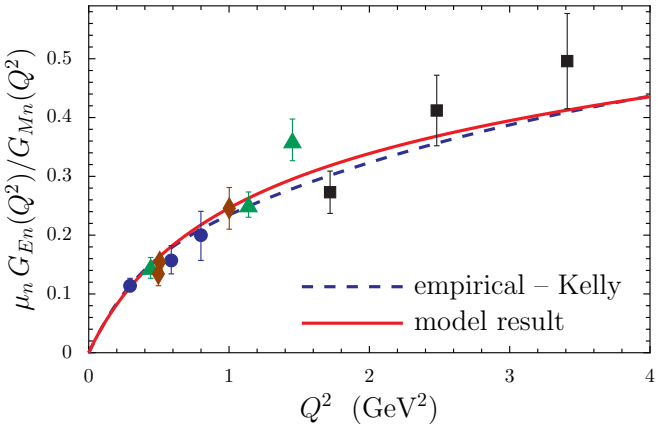

Figure 8. (Color online) Ratios of the neutron electric to magnetic Sachs form factors. The solid curve is our model result and the dashed curve is the phenomenological fit of Ref. [14]. The data are from Ref. [21].

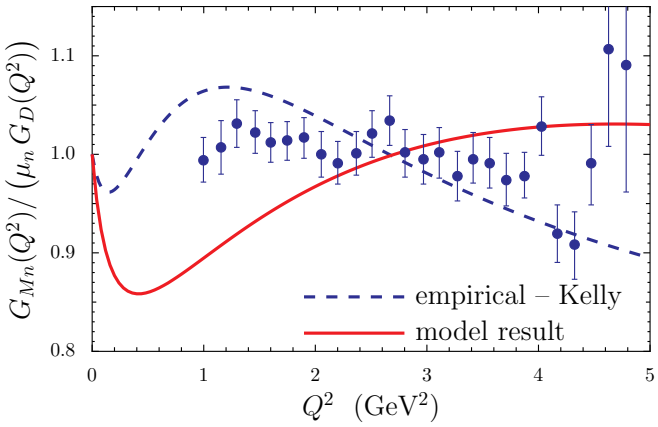

Figure 9. (Color online) The solid curve is our model result for the neutron form factors ratio of $G_{Mn}/\left(\mu_n\, G_D\right)$, where $G_D(Q^2)$ is the dipole form factor with mass parameter $\Lambda = 0.71\,\mathrm{GeV}^2$. The dashed curve is the empirical result from Ref. [14] and the data is from Ref. [22].

functions induced by using the specific forms of Eq. (6). The resulting values of the nucleon magnetic moments are also shown in the table and are in good agreement with the experimental values of $\mu_p = 2.79\,\mu_N$ and $\mu_n = -1.91\,\mu_N$ for the proton and neutron, respectively.

The results for the proton Sachs form factors are shown in Figs. 2 and 3. We find that our results agree very well, over a large Q^2 range, with the empirical parameterizations of Kelly given in Ref. [14]. At small Q^2 both the electric and magnetic form factors fall off a little too rapidly, which is a likely indication that the pion cloud component of the LFWF is slightly too large. In Figs. 4 and 5 we compare our form factor results with data for the ratios $\mu_p\, G_{Ep}(Q^2)/G_{Mp}(Q^2)$ and $Q^2\, F_{2p}(Q^2)/F_{1p}(Q^2)$, respectively. In each case our results agree very well with the measured ratios, and although not shown in Fig. 4 we find that the G_{Ep}/G_{Mp} form factor ratio crosses zero at $Q^2 \simeq 12.3\,\mathrm{GeV}^2$.

Our results for the neutron Sachs form factors are illustrated in Figs. 6 and 7. A comparison with the empirical parameterizations of Ref. [14] and the recent Jefferson Lab data for G_E^n, given in Ref. [21], shows excellent agreement. Similar to the proton case, we find that our neutron magnetic form factor falls slightly too fast for small values of Q^2. However, our agreement with the Kelly result for G_{En} is extremely good. Figs. 8 and 9 compare our form factor results with data for the ratios $\mu_n\, G_{En}(Q^2)/G_{Mn}(Q^2)$ and $G_{Mn}(Q^2)/\left[\mu_n\, G_D(Q^2)\right]$, respectively, where $G_D(Q^2)$ is the dipole form factor with mass parameter $\Lambda = 0.71\,\mathrm{GeV}^2$. The comparison between data and our model results in Fig. 8 is very good and our description of the $G_{Mn}(Q^2)$ data from Ref. [22] (see Fig. 9) is generally as good as the one provided by Kelly [14] and seems to be better for the larger values of Q^2.

The importance of looking at the separate quark sector form factors for u and d quarks in the nucleon has

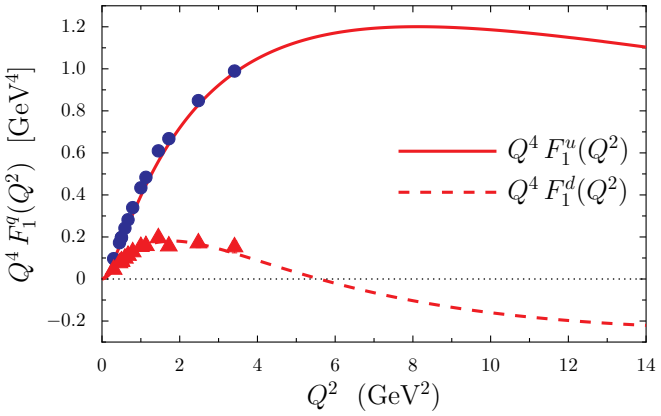

Figure 10. (Color online) Model results for the Dirac quark sector form factors F_1^u and F_1^d multiplied by Q^4. The data are from [8, 16–21, 25–29] .

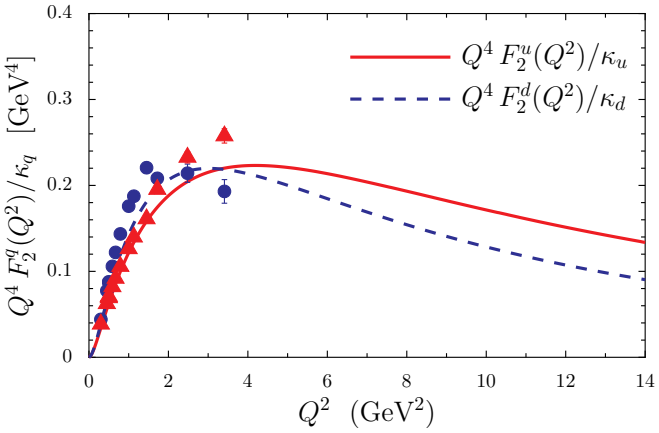

Figure 11. (Color online) Model results for the Pauli quark sector form factors F_2^u and F_2^d multiplied by Q^4. The data are from [8, 16–21, 25–29] .

been stressed in Ref. [8]. This is possible because of the charge symmetry (invariance under interchange of u and d quarks) of the nucleon wave function [23, 24]. The quark sector Dirac and Pauli form factors are defined by

$$F_{1(2)}^u = 2\,F_{1(2)p}^u + F_{1(2)n}^u \quad \& \quad F_{1(2)}^d = F_{1(2)p}^d + 2\,F_{1(2)p}^d. \tag{59}$$

We illustrate results for $Q^4\,F_1^q$ and $Q^4\,F_2^q/\kappa_q$, where $\kappa_q \equiv F_2^q(Q^2=0)$ and $q \in u,\,d$, in Figs. 10 and 11, respectively. In each case the agreement between our results and the data from Ref. [8] is very good. We predict that F_1^d has a zero-crossing at approximately 5.5 GeV^2 and also observe a cross over between F_2^u and F_2^d at approximately 3 GeV^2. This is consistent with the data in Ref. [8], where it is shown that for both the Dirac and Pauli quark sector form factors, the d quark sector drops faster than the u quark sector. The data in Ref. [8] also exhibits the behavior that on the domain $1\,\text{GeV}^2 \lesssim Q^2 \lesssim 3.4\,\text{GeV}^2$, the ratio of the Pauli to Dirac form factors, in both the u- and d-quark sectors, is almost constant.

Flavor separated form factors have been considered for a long time in the context of generalized parton distributions GPDs [30, 31]. The present work is limited to elastic form factors and benefits from the knowledge gained by eight years of experimentation, including the extension of neutron form factors to higher values of Q^2. The wave functions of our model do contain predictions related to GPDs and these will be considered in the future.

IV. PROTON SPIN CONTENT

The true test of this model is the independent prediction of the proton spin content. This prediction is implied by the definition of the flavor-spin wave function given in Eq. (8) and the LFWFs given in Eqs. (16) and (17). The helicity parton distribution functions (PDFs) are given by

$$\Delta q(x) = q_+(x) - q_-(x), \tag{60}$$

where $q_+(x)$ is the number density of quarks with helicity parallel to the nucleon spin and $q_-(x)$ is the number density of quarks with helicity anti-parallel to the nucleon spin. The quark spin content, namely $\Delta\Sigma = \Delta u + \Delta d$, is obtained by integrating Eq. (60) over x for both the u and d quarks. In this work we ignore contributions to $\Delta\Sigma$ from the heavier quark flavors.

Using the proton spin-flavor wave function of Eq. (8), we obtain

$$\Delta u(x) = \frac{3}{2}\,\Delta q_s(x) + \frac{1}{2}\,\Delta q_a(x), \tag{61}$$

$$\Delta d(x) = \Delta q_a(x), \tag{62}$$

for the bare nucleon, where the subscripts s and a refer to the contributions to the helicity PDFs from the quark–scalar-diquark and quark–axial-vector-diquark components of the nucleons LFWF. The functions $\Delta q_s(x)$ and $\Delta q_a(x)$ are completely analogous to the bare nucleon form factor quantities $f_1^s(Q^2)$ and $f_1^a(Q^2)$, respectively, and expressions can easily by obtained using Eq. (60) and the results given in Eqs. (26)-(37). We find

$$\Delta q_s(x) = \frac{Z_s}{16\pi^3}\int \frac{d^2k_\perp}{x^2(1-x)} \left[\left[(M\,x+m)\,\varphi_1^s + 2\,M\,x\,\varphi_2^s\right]^2 - k_\perp^2\,\varphi_2^{s\,2}\right], \tag{63}$$

$$\Delta q_a(x) = \frac{Z_a}{8\pi^3}\int \frac{d^2k_\perp}{x^2(1-x)} \left[\frac{1+x^2}{(1-x)^2}k_\perp^2\varphi_1^{a\,2} - \left[(M\,x+m)\varphi_1^a + 2\,M\,x\,\varphi_2^a\right]^2\right]. \tag{64}$$

The spin content is determined by the first moments of

the helicity PDFs, namely

$$\Delta u \equiv \int_0^1 dx\, \Delta u(x) = \frac{3}{2}\Delta q_s + \frac{1}{2}\Delta q_a, \tag{65}$$

$$\Delta d \equiv \int_0^1 dx\, \Delta d(x) = \Delta q_a. \tag{66}$$

The dominant terms in Eqs. (63) and (64) are those containing the nucleon mass, and these come in with a positive sign for the scalar diquark component and with a negative sign for the axial-vector piece. This implies that the quark spin content of the term with the axial-vector diquark can be expected to be negative. Importantly, these results refer to the contribution of the nucleon without including the effects of the pion cloud.

The effect of the pion cloud on the nucleon spin sum is determined by evaluating the diagrams illustrated in Fig. 1, where instead of the electromagnetic current operator we insert the quark spin operator. In this case, only the first and second diagrams in Fig. 1 contribute because the spin of the pion zero. We find that the nucleon spin sum, including the pion cloud, is given by

$$\Delta\Sigma_\pi = \left(Z_{N\pi} + \Delta q_N^\pi\right)\left(\Delta u + \Delta d\right), \tag{67}$$

where

$$\Delta q_N^\pi = -3\, g_{\pi N}^2 \int_0^1 dx \int \frac{d^2k_\perp}{2(2\pi)^3}\,(1-x) \frac{\boldsymbol{k}_\perp^2 - (1-x)^2\, M^2}{\left[\boldsymbol{k}_\perp^2 + (1-x)^2\, M^2 + x\, m_\pi^2\right]^2}\, F_{\pi N}^2(x, k_\perp^2). \tag{68}$$

Numerical evaluation using our LFWFs gives

$$\Delta u = 0.921, \qquad \Delta d = -0.424, \tag{69}$$

so that the fraction of the spin carried by the quarks in a bare nucleon is

$$\Delta\Sigma = \Delta u + \Delta d = 0.497. \tag{70}$$

Using Eq. (67) and the results

$$Z_{N\pi} = 0.706, \qquad \Delta q_N^\pi = 0.0281, \tag{71}$$

implies that the nucleon spin sum, including the effects of the pion cloud is given by

$$\Delta\Sigma_\pi = 0.365. \tag{72}$$

In contrast with previous work, the term Δq_N^π is greater that zero. This results from our relativistic treatment, and numerically arises from the cancellation of the two terms in the numerator of the integrand appearing in Eq. (68). This is a small effect. The value 0.365 is in good agreement with the central value 0.366 obtained in the global analysis (using $x_{min} = 0.001$) of Ref. [32]. Future measurements made at higher energies may reduce this central value. However, the present agreement is very good, considering that the model wave function has no gluons.

V. SUMMARY AND DISCUSSION

The main point of our work is to show that it is possible to construct a constituent quark model – capable of reproducing the measured electromagnetic form factors – in which the quark spin content of the nucleon is in qualitative agreement with experiment. This phenomenology is achieved by using relativistically moving quarks, immersed in a cloud of pions. There are several possible improvements to the model: including more pionic terms, increasing the flexibility of the guess for the wave functions given in Eq. (6), improving the treatment of the pion-nucleon vertex along the lines suggested by [33], including the effect of intermediate Δ-baryons in the pion cloud contribution and so on. While the present model is not likely to be the final word on the subject, it does show that the quark model, with suitable obvious modifications from the original non-relativistic, pion cloud-free version does survive the "proton spin crisis" in a manner very similar to that previously noted [2, 10]. Future refinements and tests of the model depend on the ability of experimentalists to make improved measurements.

ACKNOWLEDGEMENTS

This work has been partially supported by US DOE Grant No. DE-FG02-97ER-41014 and by the Australian Research Council through FL0992247 (ICC).

[1] J. Ashman *et al.* [European Muon Collaboration], Phys. Lett. B **206**, 364 (1988).
[2] A. W. Thomas, Phys. Rev. Lett. **101**, 102003 (2008) [arXiv:0803.2775 [hep-ph]].
[3] J. Arrington, K. de Jager and C. F. Perdrisat, J. Phys. Conf. Ser. **299**, 012002 (2011) [arXiv:1102.2463 [nucl-ex]].
[4] I. C. Cloët, G. Eichmann, B. El-Bennich, T. Klahn and C. D. Roberts, Few Body Syst. **46**, 1 (2009) [arXiv:0812.0416 [nucl-th]].
[5] M. R. Frank, B. K. Jennings and G. A. Miller, Phys. Rev. C **54**, 920 (1996) [nucl-th/9509030].
[6] G. A. Miller, Phys. Rev. C **66**, 032201 (2002) [nucl-th/0207007].
[7] H. H. Matevosyan, G. A. Miller and A. W. Thomas, Phys. Rev. C **71**, 055204 (2005) [nucl-th/0501044].
[8] G. D. Cates, C. W. de Jager, S. Riordan and B. Wojtsekhowski, Phys. Rev. Lett. **106**, 252003 (2011) [arXiv:1103.1808 [nucl-ex]].

[9] S. Theberge, A. W. Thomas and G. A. Miller, Phys. Rev. D **22**, 2838 (1980) [Erratum-ibid. D **23**, 2106 (1981)].

[10] F. Myhrer and A. W. Thomas, Phys. Lett. B **663**, 302 (2008) [arXiv:0709.4067 [hep-ph]].

[11] S. J. Brodsky, H. -C. Pauli and S. S. Pinsky, Phys. Rept. **301**, 299 (1998) [hep-ph/9705477].

[12] S. J. Brodsky, J. R. Hiller, D. S. Hwang and V. A. Karmanov, Phys. Rev. D **69**, 076001 (2004) [hep-ph/0311218].

[13] A. Szczurek, M. Ericson, H. Holtmann and J. Speth, Nucl. Phys. A **596**, 397 (1996) [hep-ph/9602213].

[14] J. J. Kelly, Phys. Rev. C **70**, 068202 (2004).

[15] S. Venkat, J. Arrington, G. A. Miller and X. Zhan, Phys. Rev. C **83**, 015203 (2011) [arXiv:1010.3629 [nucl-th]].

[16] M. K. Jones *et al.* [Jefferson Lab Hall A Collaboration], Phys. Rev. Lett. **84**, 1398 (2000) [nucl-ex/9910005].

[17] O. Gayou *et al.* [Jefferson Lab Hall A Collaboration], Phys. Rev. Lett. **88**, 092301 (2002) [nucl-ex/0111010].

[18] O. Gayou, K. Wijesooriya, A. Afanasev, M. Amarian, K. Aniol, S. Becher, K. Benslama and L. Bimbot *et al.*, Phys. Rev. C **64**, 038202 (2001).

[19] A. J. R. Puckett, E. J. Brash, M. K. Jones, W. Luo, M. Meziane, L. Pentchev, C. F. Perdrisat and V. Punjabi *et al.*, Phys. Rev. Lett. **104**, 242301 (2010) [arXiv:1005.3419 [nucl-ex]].

[20] A. J. R. Puckett, E. J. Brash, O. Gayou, M. K. Jones, L. Pentchev, C. F. Perdrisat, V. Punjabi and K. A. Aniol *et al.*, arXiv:1102.5737 [nucl-ex].

[21] S. Riordan, S. Abrahamyan, B. Craver, A. Kelleher, A. Kolarkar, J. Miller, G. D. Cates and N. Liyanage *et al.*, Phys. Rev. Lett. **105**, 262302 (2010) [arXiv:1008.1738 [nucl-ex]].

[22] J. Lachniet *et al.* [CLAS Collaboration], Phys. Rev. Lett. **102**, 192001 (2009) [arXiv:0811.1716 [nucl-ex]].

[23] G. A. Miller, B. M. K. Nefkens and I. Slaus, Phys. Rept. **194**, 1 (1990).

[24] G. A. Miller, A. K. Opper and E. J. Stephenson, Ann. Rev. Nucl. Part. Sci. **56**, 253 (2006) [nucl-ex/0602021].

[25] H. Zhu *et al.* [E93026 Collaboration], Phys. Rev. Lett. **87**, 081801 (2001) [nucl-ex/0105001].

[26] J. Bermuth, P. Merle, C. Carasco, D. Baumann, D. Bohm, D. Bosnar, M. Ding and M. O. Distler *et al.*, Phys. Lett. B **564**, 199 (2003) [nucl-ex/0303015].

[27] G. Warren *et al.* [Jefferson Lab E93-026 Collaboration], Phys. Rev. Lett. **92**, 042301 (2004) [nucl-ex/0308021].

[28] D. I. Glazier, M. Seimetz, J. R. M. Annand, H. Arenhovel, M. Ases Antelo, C. Ayerbe, P. Bartsch and D. Baumann *et al.*, Eur. Phys. J. A **24**, 101 (2005) [nucl-ex/0410026].

[29] B. Plaster *et al.* [Jefferson Laboratory E93-038 Collaboration], Phys. Rev. C **73**, 025205 (2006) [nucl-ex/0511025].

[30] M. Diehl, T. .Feldmann, R. Jakob and P. Kroll, Eur. Phys. J. C **39**, 1 (2005) [hep-ph/0408173].

[31] M. Guidal, M. V. Polyakov, A. V. Radyushkin and M. Vanderhaeghen, Phys. Rev. D **72**, 054013 (2005) [hep-ph/0410251].

[32] D. de Florian, R. Sassot, M. Stratmann and W. Vogelsang, Phys. Rev. Lett. **101**, 072001 (2008) [arXiv:0804.0422 [hep-ph]].

[33] M. Alberg and G. A. Miller, Phys. Rev. Lett. (2012) [arXiv:1201.4184 [nucl-th]].